DALTON
FULL PAPER

Two new bimetallic phosphido carbonyl complexes of nickel(0): $[Ni_2(CO)_2(PPh_3)_2(\mu\text{-}CO)(\mu\text{-}PPh_2)]^-$ and $[Ni_2(CO)_4(\mu\text{-}PPh_2)_2]^{2-}$

Banu Keşanlı,[a] Donna Rae Gardner,[a] Brian Scott[b] and Bryan W. Eichhorn*[a]

[a] *Department of Chemistry and Biochemistry, University of Maryland, College Park, Maryland 20742, USA*
[b] *Los Alamos National Laboratory, Chemical Sciences and Technology Division, Los Alamos, New Mexico 87545, USA*

Received 31st January 2000, Accepted 23rd February 2000
Published on the Web 30th March 2000

Toluene solutions of $Ni(CO)_2(PPh_3)_2$ react with excess potassium metal to give the $[Ni_2(CO)_4(\mu\text{-}PPh_2)_2]^{2-}$ ion (**2**) which contains two tetrahedral Ni centers fused along a common edge. Each Ni achieves an 18 electron configuration without the formation of a Ni–Ni bond (d_{Ni-Ni} = 3.397(1) Å) in contrast to the two-electron oxidation product, $Ni_2(CO)_4(\mu\text{-}PPh_2)_2$ (**1**) (d_{Ni-Ni} = 2.510(2) Å). The anion **2** shows a reversible oxidation at −1.5 V and a quasi-reversible oxidation at −1.1 V *vs.* $FeCp_2/FeCp_2^+$. The negative ion electrospray mass spectrum of **2** shows the one-electron oxidation product of **2**, $[Ni_2(CO)_4(\mu\text{-}PPh_2)_2]^-$, along with three decarbonylation products $[Ni_2(CO)_3(\mu\text{-}PPh_2)_2]^-$, $[Ni_2(CO)_2(\mu\text{-}PPh_2)_2]^-$, and $[Ni_2(CO)(\mu\text{-}PPh_2)_2]^-$ where $[Ni_2(CO)_3(\mu\text{-}PPh_2)_2]^-$ is the base peak. Ethylenediamine solutions of Sn_9^{4-} react with $Ni(CO)_2(PPh_3)_2$ in the presence of 2,2,2-crypt (4,7,13,16,21,24-hexaoxa-1,10-diazabicyclo-[8.8.8]hexacosane) to reproducibly give $[Ni_2(CO)_2(PPh_3)_2(\mu\text{-}CO)(\mu\text{-}PPh_2)]^-$ (**3**), as one of three products. The anion **3** also has an edge-shared bitetrahedral geometry but, unlike **2**, possesses a Ni–Ni bond (d_{Ni-Ni} = 2.4930(9) Å).

Introduction

The synthesis of mononuclear and bimetallic phosphido complexes of the Group 10 metals was first investigated by Issleib, Rettkowski and Hayter in the 1960's[1–3] and is still of current interest.[4–6] These and subsequent studies have revealed a variety of synthetic entries into bimetallic Ni phosphido complexes that include (i) oxidative addition of diphosphines ($R_2P\text{–}PR_2$) to zero valent Ni precursors,[2,7] (ii) phosphido-for-halide metathesis using R_2P^- salts and Ni halides,[8,9] (iii) reactions of nickel carbonyl anions with dialkyl phosphorus halides[9] and (iv) decomposition of coordinated phosphine ligands under reducing conditions.[10–12] The resulting compounds usually contain tetrahedral Ni in the +1 oxidation state and all possess Ni–Ni single bonds ($d_{Ni-Ni} \approx 2.50$ Å) to achieve 18-electron configurations.[8–10,13,14] One of the earliest examples of type (i) chemistry was the preparation of $Ni_2(CO)_4(\mu\text{-}PPh_2)_2$ (**1**) from $Ni(CO)_4$ and Ph_2PPPh_2 in refluxing mesitylene (eqn. (1)).[2] The

$$2\ Ni(CO)_4 + Ph_2PPPh_2 \longrightarrow \underset{\mathbf{1}}{Ni_2(CO)_4(\mu\text{-}PPh_2)_2} + 4\ CO \quad (1)$$

crystal structure[15] of **1** revealed two tetrahedrally coordinated Ni(I) metal ions separated by 2.506 Å and symmetrically bridged by the two phosphido ligands. Other compounds, such as $(CO)_2Ni(\mu\text{-}P(t\text{-}Bu)_2)_2Ni(CO)$ and $(PR_3)Ni(\mu\text{-}P(SiMe_3)_2)_2\text{-}Ni(PR_3)$ where R = Me, Et, n-Bu, i-Bu, C_6H_{11}, and Ph contain, three coordinate metal centers and Ni–Ni bonds.[8,9]

Issleib and Rettkowski have shown[3] that reactions of $Ni(CO)_4$ with R_2P^- salts under photolytic conditions give monomeric anions of formula $[Ni(CO)_3PPh_2]^-$ and $[Ni(CO)_2\text{-}(PPh_2)]^{2-}$. Schaefer and Binder also prepared several mononuclear phosphido complexes by similar routes.[16,17]

We report here the synthesis, structure and properties of two new carbonyl–phosphido bimetallic compounds, $[Ni_2(CO)_4\text{-}(\mu\text{-}PPh_2)_2]^{2-}$ (**2**) and $[Ni_2(CO)_2(PPh_3)_2(\mu\text{-}CO)(\mu\text{-}PPh_2)]^-$ (**3**), that contain zero-valent Ni and different metal–metal bond orders. The latter is obtained from an unusual electron transfer reaction from a Zintl ion and the former is the formal two-electron reduction product of **1**. The electrochemical generation of **2** was cited by Dessy *et al.* several years ago,[18] however, isolation and characterization of the ion was not accomplished at that time. Our study addresses the electrochemical conversions of **1** and **2**, their gas phase behavior and provides a structural and spectroscopic comparison of the compounds.

Results

Synthesis and characterization

Toluene solutions of $Ni(CO)_2(PPh_3)_2$ react with excess potassium metal in the presence of 2,2,2-crypt (4,7,13,16,21,24-hexaoxa-1,10-diazabicyclo[8.8.8]hexacosane) to give $[Ni_2(CO)_4\text{-}(\mu\text{-}PPh_2)_2]^{2-}$ (**2**) as a microcrystalline $[K(2,2,2\text{-crypt})]^+$ salt in 63% yield (eqn. (2)). The chemistry of eqn. (2) does not proceed

$$2\ Ni(CO)_2(PPh_3)_2 + 4\ K + 2(2,2,2\text{-crypt}) \longrightarrow \underset{\mathbf{2}}{[Ni_2(CO)_4(\mu\text{-}PPh_2)_2]^{2-}} + 2[K(2,2,2\text{-crypt})]^+ + 2\ KPh + 2\ PPh_3 \quad (2)$$

in the absence of 2,2,2-crypt. The phenyl containing byproduct in eqn. (2) is presumably KPh (*cf.* $NaPPh_2$ synthesis).[19] The salt of **2** is reddish brown in solution, red in the solid state and decomposes upon exposure to air.

The salt has been characterized by IR and NMR spectroscopic studies (^{31}P, ^1H), electrochemical studies and negative ion electrospray mass spectrometry (NI-EMS). The single crystal X-ray structure of this salt has been determined but, due to the weakness of the diffraction data, the refinement was not satisfactory (see below).

When eqn. (2) chemistry is conducted in mixed dmf/ethylenediamine solvents with NaK alloys, poor yields of a highly solvated $[K(2,2,2\text{-crypt})]^+$ salt of **2** are formed having the formula $[K(2,2,2\text{-crypt})]_2[Ni_2(CO)_4(\mu\text{-}PPh_2)_2]\cdot 2en\cdot 2dmf$. Although this synthetic method is not convenient for preparatory scale syntheses of **2**, this crystalline form provides superior X-ray diffraction data.

Table 1 Crystallographic data for $[K(2,2,2\text{-crypt})]_2$**[2]**·2dmf·2en and [K(2,2,2-crypt)][**3**]

	$[K(2,2,2\text{-crypt})]_2$**[2]**·2dmf·2en	[K(2,2,2-crypt)][**3**]
Empirical formula	$C_{72}H_{114}K_2N_8Ni_2O_{18}P_2$	$C_{69}H_{76}KN_2Ni_2O_9P_3$
Formula weight	1637.27	1326.75
T/K	193(1)	203(2)
λ/Å	0.71073	0.71073
Space group	$P\bar{1}$	$P2_1/n$
Crystal system	Triclinic	Monoclinic
a/Å	11.211(4)	13.2760(10)
b/Å	13.861(2)	25.750(2)
c/Å	13.942(2)	19.392(2)
α/°	76.55(1)	
β/°	82.76(2)	91.464
γ/°	80.78(2)	
V/Å^3, Z	2071.0(9), 1	6627.1(10), 4
μ/mm^{-1}	0.662	0.760
Reflections collected	8573	10369
Independent reflections	7229 [R(int) = 0.0253]	8561 [R(int) = 0.0311]
Final R indices [$F > 4\sigma(F)$], $R(F)$	0.0691	0.0526
$wR(F^2)$	0.1735	0.1167

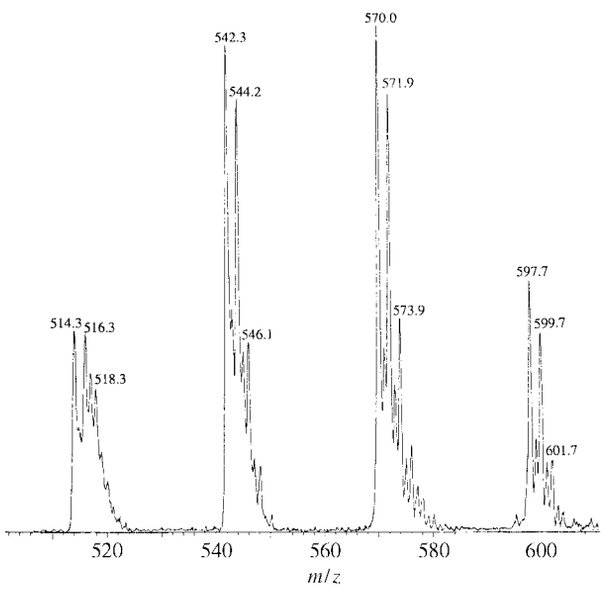

Fig. 1 Negative ion electrospray mass spectrum of $[Ni_2(CO)_4(\mu\text{-}PPh_2)_2]^{2-}$ recorded from dmf solutions. The oxidized parent ion $[Ni_2(CO)_4(\mu\text{-}PPh_2)_2]^-$ ($m/z = 600$) and successive decarbonylation products $[Ni_2(CO)_3(\mu\text{-}PPh_2)_2]^-$ (base peak, $m/z = 570$), $[Ni_2(CO)_2(\mu\text{-}PPh_2)_2]^-$ ($m/z = 542$) and $[Ni_2(CO)(\mu\text{-}PPh_2)_2]^-$ ($m/z = 514$) are the prominent peaks.

Oxidation of **2** with two equivalents of Ag^+ gives several carbonyl-containing products. The neutral compound **1** is a small component of the reaction mixture. Oxidation of **2** in air does not afford any detectable quantities of **1**.

The NI-EMS studies of the non-solvated $[K(2,2,2\text{-crypt})]^+$ salt of **2** were conducted in dmf solutions at room temperature. A typical spectrum is shown in Fig. 1. There are several informative features in the mass spectrum. First, the one-electron oxidation product of **2**, the $[Ni_2(CO)_4(\mu\text{-}PPh_2)_2]^-$ ion (**4**), is clearly evident at $m/z = 598$ u whereas the peak for the unoxidized dianion **2** ($m/z = 299$ u) is very weak or absent. This observation provides insight into the redox properties of **2** that will be discussed in the electrochemistry section. Second, the decarbonylation products of **4**; namely $[Ni_2(CO)_3(\mu\text{-}PPh_2)_2]^-$ ($m/z = 570$ u), $[Ni_2(CO)_2(\mu\text{-}PPh_2)_2]^-$ ($m/z = 542$ u) and $[Ni_2(CO)(\mu\text{-}PPh_2)_2]^-$ ($m/z = 514$ u) are prominent ions in the spectrum. The spectral base peak is the tricarbonyl anion $[Ni_2(CO)_3(\mu\text{-}PPh_2)_2]^-$.

Ethylenediamine solutions of Sn_9^{4-} and $Ni(CO)_2(PPh_3)_2$ react in the presence of 2,2,2-crypt to reproducibly give at least three different products; the reported Sn_9^{3-} ion,[20] [*closo*-$HSn_9Ni_2(CO)_2]^{3-}$,[21] and $[Ni_2(CO)_2(PPh_3)_2(\mu\text{-}CO)(\mu\text{-}PPh_2)]^-$ (**3**). All three products have been isolated as the $[K(2,2,2\text{-crypt})]^+$ salts and crystallographically characterized but only **3** will be described here. The salt of **3** is formed in low yield (<10% based on Ni) in these reactions as pale orange-red air-sensitive crystals. The crystals were manually separated from the reaction mixture and characterized by single crystal X-ray diffraction.

Table 2 Selected bond distances (Å) and angles (°) for $[Ni_2(CO)_4(\mu\text{-}PPh_2)_2]^{2-}$

Ni–C(2)	1.746(6)	Ni–P(1)′	2.300(2)
Ni–C(1)	1.751(6)	C(1)–O(1)	1.148(7)
Ni–P(1)	2.2905(14)	C(2)–O(2)	1.155(7)
C(2)–Ni–C(1)	118.7(3)	P(1)–Ni–P(1)′	84.59(5)
C(2)–Ni–P(1)	110.1(2)	Ni–P(1)–Ni′	95.41(5)
C(1)–Ni–P(1)	108.9(2)	O(1)–C(1)–Ni	176.2(5)
C(2)–Ni–P(1)′	116.5(2)	O(2)–C(2)–Ni	175.6(5)
C(1)–Ni–P(1)′	112.5(2)		

Structural studies

$[Ni_2(CO)_4(\mu\text{-}PPh_2)_2]^{2-}$ (2). The single crystal X-ray structure of the red crystals isolated from the synthesis of **2** from toluene solvent (eqn. (2)) are monoclinic, space group $P2_1/n$, with $a = 15.915$ Å, $b = 17.715$ Å, $c = 25.582$ Å and $\beta = 102.9°$. The structure contains isolated $[K(2,2,2\text{-crypt})]^+$ ions and the anion **2**, however, the diffraction data from these crystals were weak and the refinement was of low quality. The structure of the solvated form (see below) was far superior and the metric parameters of the $[Ni_2(CO)_4(\mu\text{-}PPh_2)_2]^{2-}$ ion were identical to the unsolvated form within experimental error. Therefore, the details of the monoclinic structure will not be discussed further.

The solvated form of $[K(2,2,2\text{-crypt})]^+$ salt of **2** is triclinic, space group $P\bar{1}$, and contains two en and two dmf solvate molecules per anion. An ORTEP drawing of **2** is shown in Fig. 2 and a summary of the crystallographic data is given in Table 1. Selected bond distances and angles are listed in Table 2. The anion resides on the crystallographic inversion center located midway between the two Ni atoms and the two μ-PPh_2 ligands. The ion has virtual D_{2d} point symmetry but only the inversion center is crystallographically imposed. The Ni atoms are in distorted tetrahedral environments with C–Ni–C, P–Ni–P, and P–Ni–C angles of 118.7(3)°, 84.59(5)°, and 112(4)° respectively. The two NiL_4 tetrahedra share a common edge

Table 3 Average bond distances (Å) and angles (°) for $Ni_2(CO)_4(\mu\text{-}PPh_2)_2$ (**1**), and $[Ni_2(CO)_4(\mu\text{-}PPh_2)_2]^{2-}$ (**2**)

	1	**2**
Ni–Ni	2.510(2)	3.397(1)
Ni–C	1.79(2)	1.75(1)
Ni–P	2.19(1)	2.30(1)
C–O	1.13(2)	1.15(1)
C–Ni–C′	117(2)	118.7(3)
C–Ni–P	107(3)	112(4)
P–Ni–P′	110(1)	84.59(5)
Ni–P–Ni′	70(1)	95.41(5)
O–C–Ni	177(1)	176(1)
Ni–P–C(Ph)	121(2)	116(3)

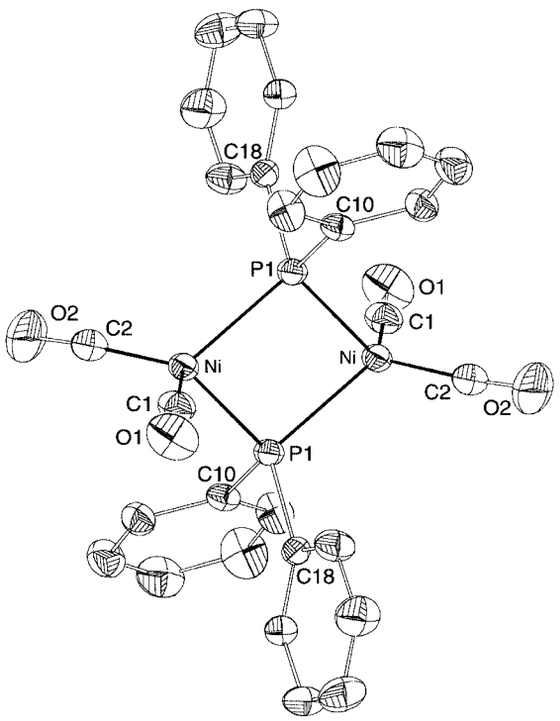

Fig. 2 ORTEP[31] drawing of the $[Ni_2(CO)_4(\mu\text{-}PPh_2)_2]^{2-}$ anion, **2**.

defined by the two symmetrically bridging μ-PPh_2 ligands with Ni–P distances of 2.30(1) Å (av). The Ni–C distances average 1.75(1) Å.

A comparison of the geometrical parameters of **2** and its neutral Ni(I) analog $Ni_2(CO)_4(\mu\text{-}PPh_2)_2$ (**1**)[15] is given in Table 3. Although the structures of **1** and **2** are quite similar, there are two important differences. First, the Ni–Ni bond in **1** (d_{Ni-Ni} = 2.510(2) Å)[15] is notably absent in **2** (d_{Ni-Ni} = 3.397(1) Å) as expected. As a result, the Ni–P–Ni angles are much less acute in **2** in comparison to **1** (see Table 3) and other phosphido-bridged dinickel compounds containing Ni–Ni bonds.[22–24] The second difference is the slight but significant variations in Ni–P and Ni–C bond distances in the two compounds. The Ni–P distances of **2** are longer than those of **1** whereas the Ni–C distances are shorter. The latter are consistent with lower Ni oxidation state and higher negative charge in **2** and are also consistent with the trends in ν(CO) values. The elongated Ni–P bonds in **2** may be due, in part, to the long Ni–Ni separation and larger Ni–P–Ni bond angles rather than the differences in formal Ni oxidation state and anionic charge. For comparison, the Ni–P contacts in the anionic zero-valent ion **3**, which contains a Ni–Ni bond (described in the next section), are more similar to the neutral nickel(I) complex **1**.

The $[K(2,2,2\text{-crypt})]^+$ ion in the lattice was crystallographically well behaved with metric parameters that are similar to other structurally characterized compounds. The solvate molecules were well separated from the cations and anions but disorder was present in both cases.

Table 4 Selected bond distances (Å) and angles (°) for $[Ni_2(CO)_2(PPh_3)_2(\mu\text{-}CO)(\mu\text{-}PPh_2)]^-$

Ni(1)–C(49)	1.746(6)	Ni(2)–C(51)	1.901(5)
Ni(1)–C(51)	1.940(5)	Ni(2)–P(2)	2.170(2)
Ni(1)–P(1)	2.184(2)	Ni(2)–P(3)	2.229(2)
Ni(1)–P(3)	2.2344(14)	O(1)–C(49)	1.152(6)
Ni(1)–Ni(2)	2.4930(9)	O(2)–C(50)	1.149(6)
Ni(2)–C(50)	1.749(6)	O(3)–C(51)	1.168(6)
C(49)–Ni(1)–C(51)	108.6(2)	C(50)–Ni(2)–P(3)	120.3(2)
C(49)–Ni(1)–P(1)	104.6(2)	C(51)–Ni(2)–P(3)	106.1(2)
C(51)–Ni(1)–P(1)	101.6(2)	P(2)–Ni(2)–P(3)	110.65(6)
C(49)–Ni(1)–P(3)	114.8(2)	Ni(2)–P(3)–Ni(1)	67.91(4)
C(51)–Ni(1)–P(3)	104.6(2)	O(1)–C(49)–Ni(1)	174.0(5)
P(1)–Ni(1)–P(3)	121.38(6)	O(2)–C(50)–Ni(2)	176.4(5)
C(50)–Ni(2)–C(51)	107.0(2)	O(3)–C(51)–Ni(2)	140.3(4)
C(50)–Ni(2)–P(2)	110.2(2)	O(3)–C(51)–Ni(1)	138.8(4)
C(51)–Ni(2)–P(2)	100.6(2)	Ni(2)–C(51)–Ni(1)	80.9(2)

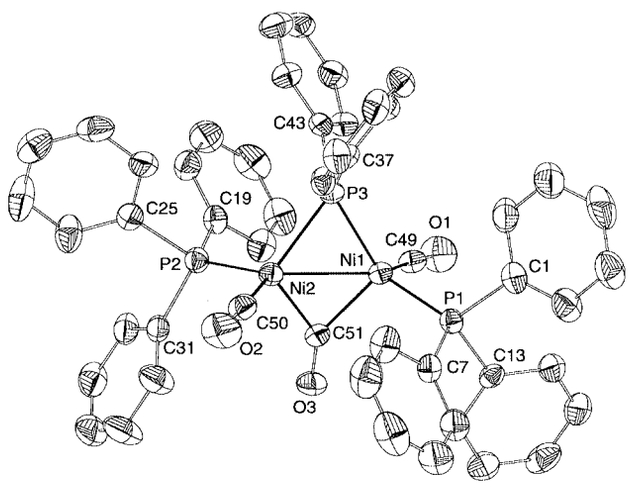

Fig. 3 ORTEP drawing of the $[Ni_2(CO)_2(PPh_3)_2(\mu\text{-}PPh_2)(\mu\text{-}CO)]^-$ anion, **3**.

$[Ni_2(CO)_2(PPh_3)_2(\mu\text{-}CO)(\mu\text{-}PPh_2)]^-$ (3)

An ORTEP drawing of **3** is shown in Fig. 3 and a summary of the crystallographic data is given in Table 1. A listing of selected bond distances and angles is given in Table 4.

The $[K(2,2,2\text{-crypt})]^+$ salt of **3** is monoclinic, space group $P2_1/c$. The anion contains two tetrahedral Ni centers fused along a common edge defined by the μ-CO and μ-PPh_2 ligands. Each Ni also contains a terminal CO (d_{Ni-C} = 1.75(1) Å, av) and a terminal PPh_3 (d_{Ni-P} = 2.18(1) Å, av). The complex possesses virtual C_2 point symmetry with a two-fold rotation axis defined by the bridging C and P atoms. In contrast to the structure of **2**, anion **3** contains a metal–metal bond as evidenced by the Ni–Ni separation of 2.4930(9) Å. The combination of the μ-PPh_2 and μ-CO ligands in **3** result in two fewer electrons per ion in comparison to the two μ-PPh_2 ligands in **2**.

Due to the short Ni–Ni separation, the Ni–P–Ni angle for the μ-PPh_2 ligand is acute (67.91°) and the Ni–P distances shortened (2.23(1) Å, av) relative to **2**. As mentioned previously, metric parameters are more similar to those of the Ni(I) compound **1**[15] than those of the anionic Ni(0) complex **2**.

Spectroscopic studies

The ^{31}P NMR spectrum of $[Ni_2(CO)_4(\mu\text{-}PPh_2)_2]^{2-}$ displays a single peak at δ −31.4 for the PPh_2 groups bridging the nickel

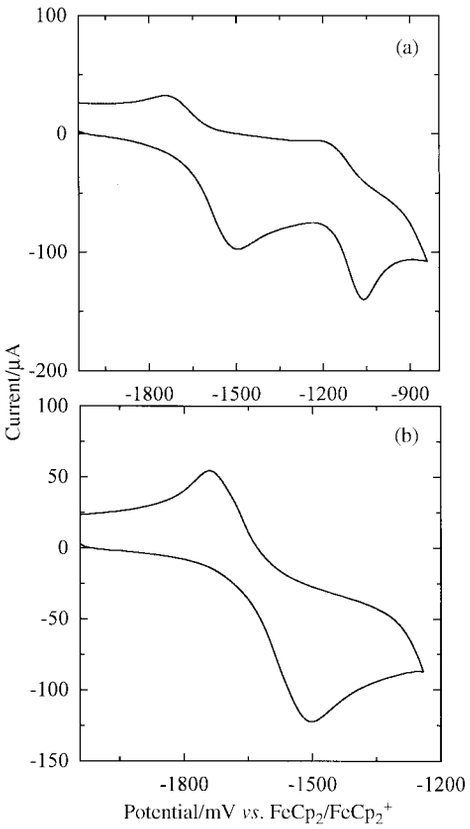

Fig. 4 (a) Cyclic voltammogram of the $[Ni_2(CO)_4(\mu\text{-}PPh_2)_2]^{2-}$ ion recorded at 500 mV s^{-1} in dmf solution. (b) Cyclic voltammogram of the −2.1 V to −1.2 V region showing the reversible oxidation at −1.5 V.

atoms. The chemical shift is similar to other metal dimers without metal–metal bonds.[25] For example, the μ-PPh_2 ligands in the metal–metal bonded iron dimer $Fe_2(CO)_6(\mu\text{-}PPh_2)_2$ appear at δ 142.8 (^{31}P NMR) whereas the non-bonded dianion $[Fe_2(CO)_6(\mu\text{-}PPh_2)_2]^{2-}$ gives μ-PPh_2 chemical shifts of δ −62.4.[26] The IR spectrum of **2** shows bands at 1904 and 1846 cm^{-1} for the stretching modes of the terminal CO groups. There is a decrease in carbonyl frequency of **2** compared to neutral compound **1** (CO = 2032 and 2003 cm^{-1}) due to an increase in π-backbonding as expected on the basis of oxidation state and charge considerations.

Electrochemistry and EPR studies

Electrochemical studies of **2** were conducted in dmf solutions at 25 °C containing 0.15 M *n*-Bu_4NPF_6 supporting electrolyte. The cyclic voltammograms of **2** show two waves at negative potential as illustrated in Fig. 4a. The general peak positions are similar to those of Dessy *et al.* after correction for the different electrochemical references.[18] The first is a reversible one-electron oxidation (see Fig. 4b) at −1.5 V (ΔE_{peak} = 0.25 V) whereas the second appears to be a multielectron quasi-reversible oxidation at −1.1 V (ΔE_{peak} = 0.14 V). For reference, the $FeCp_2/FeCp_2^+$ couple is defined as 0.0 V and has a ΔE_{peak} = 0.23 V at scan rates of 0.5 V s^{-1}. The ΔE_{peak} value of the second oxidation and its anodic current relative to the first oxidation ($i_{p,a}2^{nd}/i_{p,a}1^{st}$ = 1.7) indicate that it is not a simple one-electron process. Additional oxidation waves were not observed to the solvent cutoff at ≈+1.5 V.

The EPR spectra of electrolyzed solutions of **2** and singly oxidized solutions of **2** (reactions with one equiv of Ag^+) were measured at room temperature in dmf. A typical spectrum is shown in Fig. 5. The spectra show many signals which contain a broad single resonance at g = 1.9995 with two flanking signals separated by 98 G. These three features were always present in the EPR spectra, regardless of preparatory method, but their relative integral intensities were sample dependent.

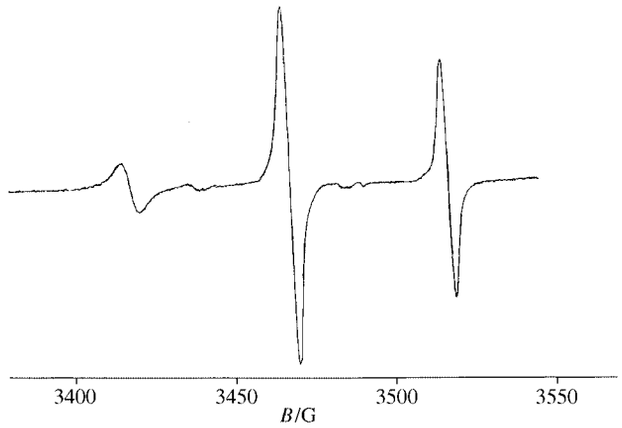

Fig. 5 EPR spectrum of oxidized samples of the $[Ni_2(CO)_4(\mu\text{-}PPh_2)_2]^{2-}$ ion recorded in dmf solution at room temperature.

Discussion

The two-step oxidation process of **2** is outlined in eqn. (3). The

$$\underset{\mathbf{2}}{[Ni_2(CO)_4(\mu\text{-}PPh_2)_2]^{2-}} \rightleftharpoons \underset{\mathbf{4}}{[Ni_2(CO)_4(\mu\text{-}PPh_2)_2]^{-}} \rightleftharpoons \underset{\mathbf{1}}{Ni_2(CO)_4(\mu\text{-}PPh_2)_2} \quad (3)$$

first oxidation can be assigned to the formation of the Ni(0)/Ni(I) species $[Ni_2(CO)_4(\mu\text{-}PPh_2)_2]^-$ (**4**), followed by a second oxidation to the neutral complex **1**. This two step oxidation is consistent with our electrochemical studies as well as those of Dessy *et al.*[18] The radical anion **4** was directly observed in the NI-EMS studies and is implicated by the EPR experiments. However, we find that the radical anion **4** is of limited stability and secondary reactions are detectable by both EPR studies and cyclic voltammetry. Bulk electrolysis of **2** was conducted at constant potential (−0.7 V) in order to generate solutions of **1**. Chemical oxidations of **2** with one and two equiv of Ag^+ were also conducted. The EPR spectra of all of these solutions showed at least two species but in different relative concentrations. Moreover, the second oxidation of **2** (*i.e.* the oxidation of **4**) is quasi-reversible at 500 mV s^{-1} with ΔE_{peak} and an anodic current indicative of a multi-electron process. Bulk electrolysis and attempts to chemically oxidize **2** with two equiv of Ag^+ give **1** as a minor product as determined by IR analysis of the reaction mixture.

One explanation of these data is that **4** undergoes secondary reactions to give EPR active by-products that are oxidized near the second oxidation wave of **2**. Although **1** and **2** can clearly be interconverted electrochemically and chemically, it appears that the interconversions are not quantitative under our experimental conditions and are complicated by side reactions. The formation of **3** from the same $Ni(CO)_2(PPh_3)_2$ precursor also suggests that several different reaction pathways may be operative in the redox chemistry of these compounds.

It is interesting to compare the chemical and electrochemical interconversions of **1** and **2** with those of the related diiron complexes $Fe_2(CO)_6(\mu\text{-}PPh_2)_2$ (**5**), and $[Fe_2(CO)_6(\mu\text{-}PPh_2)_2]^{2-}$ (**6**) reported by Collman *et al.*[26] In the diiron system, **5** and **6** are reversibly interconverted by a single two-electron oxidation indicating that the radical monoanion $[Fe_2(CO)_4(\mu\text{-}PPh_2)_2]^-$ is unstable with respect to disproportionation. The cyclic voltammetry of that system is electrode dependent. The use of Pt working electrodes resulted in irreversibility of the system, presumably due to chemisorption to the electrode surface. It is quite possible that the quasi-reversibility of the second

oxidation wave may also be due to an adsorption problem. Regardless, it appears that the oxidation of **2** occurs in successive one-electron processes in contrast to the concerted two-electron process in the diiron system.

Summary

We have studied the synthesis, structure and properties of the $[Ni_2(CO)_4(\mu\text{-}PPh_2)_2]^{2-}$ complex **2** and its electrochemical interconversion with $Ni_2(CO)_4(\mu\text{-}PPh_2)_2$, **1**. In addition, the synthesis and structure of $[Ni_2(CO)_2(PPh_3)_2(\mu\text{-}CO)(\mu\text{-}PPh_2)]^-$, **3**, is presented. The structure of **2** is virtually identical to that of **1** except the Ni–Ni bond is absent in the former. Both **1** and **2** are isolable and electrochemically interconvertable, however, the electrochemical interconversions do not appear to be quantitative. In contrast to the single-step two-electron redox process observed in the $Fe_2(CO)_6(\mu\text{-}PPh_2)_2/[Fe_2(CO)_6(\mu\text{-}PPh_2)_2]^{2-}$ couple, the electrochemical interconversions of **1** and **2** occur in two, one-electron steps.

Experimental

General operating procedures for our laboratory have been published elsewhere.[27] $Ni(CO)_2(PPh_3)_2$ was purchased from Aldrich and used without further purification. Cyclic voltammetry and bulk electrolysis were carried out with a Bioanalytical Systems BAS-100a at 25 °C. The samples were prepared in a dry box and placed into an air tight three electrode glass cell. The sample solution for cyclic voltammetry was 1.7 mM in **2** and 0.15 M in the supporting electrolyte, n-Bu_4NPF_6. A gold working electrode, Ag/AgCl reference and Pt auxiliary electrodes were used in the electrochemical measurements. Cyclic voltammograms were run at a 500 mV s^{-1} scan rate and referenced to an internal ferrocene standard (0.0 V). Bulk electrolysis of $[Ni_2(CO)_4(\mu\text{-}PPh_2)_2]^{2-}$ to form the neutral $Ni_2(CO)_4(\mu\text{-}PPh_2)_2$ was run at constant potential (−700 mV, Pt mesh electrode) in dmf with 0.13 M n-Bu_4NPF_6 as the electrolyte. A Bruker 200D-SRC EPR Spectrometer was used for the EPR analysis. Samples were drawn into 50 μL capillaries in a dry box and sealed at the top and bottom. The sealed capillaries were then placed within standard 3 mm internal diameter quartz EPR tubes. The *g* value was calculated[28] by comparing the signal of the sample to the diphenylpicrylhydrazyl standard ($g = 2.0036$). Electrospray mass spectra were recorded from dmf solution on a Finnigan mass spectrometer through direct injection. The samples were ionized by using an ESI probe and detected in the negative mode. IR spectra were recorded from KBr pellets on a Nicolet 560 FTIR spectrometer under N_2 purge. Ambient-temperature ^1H (400.136 MHz) NMR and ^{31}P (161.967 MHz) NMR spectra were recorded on a Bruker DRX400. The ^{31}P NMR data were referenced against an external 85% H_2PO_4/CD_2Cl_2 standard (0 ppm).

Syntheses

Preparation of $[K(2,2,2\text{-crypt})]_2[Ni_2(CO)_4(\mu\text{-}PPh_2)_2]$. In a dry box, $Ni(CO)_2(PPh_3)_2$ (50 mg, 0.078 mmol) and 2,2,2-crypt (29.4 mg, 0.078 mmol) were dissolved in toluene (*ca.* 3 ml) at *ca.* 40 °C. Excess K metal (6.12 mg, 0.16 mmol) was added into the yellow solution and the reaction mixture was stirred for 15 min producing a dark red precipitate. The solvent was removed, and the solid was dried under vacuum yielding a dark brown powder. The powder was redissolved in a dmf/en mixture (1 : 1, v : v), filtered through tightly packed glass wool in a pipet. After 24 h red crystals were formed in the reaction vessel. Yield: 35 mg (63%). IR (KBr pellet) 1904 (s), 1846 cm^{-1} (s). ^1H NMR (DMSO-d_6): δ 7.4–6.6 (PPh_2). $^{31}P\{^1H\}$ NMR (DMSO-d_6): δ −31.4.

Preparation of $[K(2,2,2\text{-crypt})]_2[Ni_2(CO)_4(\mu\text{-}PPh_2)_2]\cdot 2dmf\cdot 2en$. $Ni(CO)_2(PPh_3)_2$ (42 mg, 0.066 mmol), 2,2,2-crypt (100 mg, 0.26 mmol) and Na/K (5 mg) were stirred in a dmf/en mixture (1 : 1, v : v) (*ca.* 4 mL) until all Na/K was dissolved. The reaction mixture was filtered through tightly packed glass wool in a pipet and concentrated *in vacuo* to 2 mL. A few red crystals were formed in the reaction vessel after 24 h.

Preparation of $[K(2,2,2\text{-crypt})][Ni_2(CO)_2(PPh_3)_2(\mu\text{-}CO)(\mu\text{-}PPh_2)]$. $Ni(CO)_2(PPh_3)_2$ (42 mg, 0.066 mmol), K_4Sn_9 (81 mg, 0.066 mmol) and 2,2,2-crypt (100 mg, 0.26 mmol) were dissolved in en (*ca.* 4 ml) and stirred for 4 h yielding a dark red solution. The reaction mixture was filtered through tightly packed glass wool in a pipet and concentrated *in vacuo* to 2 mL. After 3 weeks, the reaction vessel contained three different crystals; pale orange-red blocks, large dark brown blocks and dark brown needles. The pale orange-red crystals were removed from the mother-liquor, washed with toluene and dried *in vacuo*.

Oxidation of 2. dmf solutions of **2** were reacted with 1 or 2 equiv of $AgBF_4$ in the drybox. Solutions were stirred for 30 min, evaporated to dryness and characterized by EPR and IR spectroscopy.

Crystallography

$[K(2,2,2\text{-crypt})]_2[Ni_2(CO)_4(\mu\text{-}PPh_2)_2]\cdot 2dmf\cdot 2en$. A dark red block was mounted on a thin glass fiber using silicone grease. The crystal data were collected at 193(1) K under an N_2 vapour stream on a Siemens P4/PC diffractometer. The lattice parameters were optimized from a least-squares calculation on 32 carefully centered reflections of high Bragg angle. The data were collected using ω scans with a 0.70° scan range. Three check reflections monitored every 97 reflections showed no systematic variation of intensities. The structure refinement was performed using SHELX 93 software.[29,30] The data were affected by absorption and were not corrected. The results are summarized in Table 1.

$[K(2,2,2\text{-crypt})][Ni_2(CO)_2(PPh_3)_2(\mu\text{-}CO)(\mu\text{-}PPh_2)]$. A reddish-orange block was mounted and its cell parameters determined as described above. The data were collected using ω scans with a 1.0° scan range. Three check reflections monitored every 97 reflections showed no systematic variation of intensities. Space group determination, data collection and data reduction were performed as above. Data were not corrected for absorption. The results are summarized in Table 1.

CCDC reference number 186/1883.

See http://www.rsc.org/suppdata/dt/b0/b000852o/ for crystallographic files in .cif format.

Acknowledgements

This work was funded by the National Science Foundation through grant CHE-9500686. We thank Jeff Blankman and Professor Robert Pilato for help with the electrochemical experiments and Professor Neil Blough for help with the EPR spectroscopy.

References

1 R. G. Hayter, *Inorg. Chem.*, 1963, **2**, 1031.
2 R. G. Hayter, *Inorg. Chem.*, 1964, **3**, 711.
3 K. Issleib and W. Rettkowski, *Z. Naturforsch.*, *Teil B*, 1966, **21**, 999.
4 C. Mealli, A. Ienco, A. Galindo and E. P. Carreno, *Inorg. Chem.*, 1999, **38**, 4629.
5 P. Leoni, G. Pieri and M. Pasquali, *J. Chem. Soc.*, *Dalton Trans.*, 1998, 657.
6 P. Leoni, S. Papucci and M. Pasquali, *Polyhedron*, 1998, **17**, 3145.
7 J. Chatt and D. T. Thompson, *J. Chem. Soc.*, 1964, 1005.
8 H. Schaefer and D. Binder, *Z. Anorg. Allg. Chem.*, 1987, **546**, 55.
9 A. M. Arif, R. A. Jones and S. T. Schwab, *J. Coord. Chem.*, 1987, **16**, 51.

10 C. G. Nobile, G. Vasapollo, P. Giannoccaro and A. Sacco, *Inorg. Chim. Acta*, 1981, **48**, 261.
11 R. Giannandrea, P. Mastrorilli, C. F. Nobile and U. Englert, *J. Chem. Soc.*, *Dalton Trans.*, 1997, 1355.
12 N. Mezailles, P. L. Floch, K. Waschbusch, L. Ricard, F. Mathey and C. P. Kubiak, *J. Organomet. Chem.*, 1997, **541**, 277.
13 A. M. Arif, D. J. Chandler and R. A. Jones, *J. Coord. Chem.*, 1988, **17**, 45.
14 B. L. Barnett and C. Krueger, *Cryst. Struct. Commun.*, 1973, **2**, 85.
15 J. A. J. Jarvis, R. H. B. Mais, P. G. Owston and D. T. Thompson, *J. Chem. Soc. A*, 1970, 1867.
16 H. Schaefer, *Z. Anorg. Allg. Chem.*, 1979, **459**, 157.
17 H. Schaefer and D. Binder, *Z. Anorg. Allg. Chem.*, 1987, **546**, 79.
18 R. E. Dessy, R. Kornmann, C. Smith and R. Hayter, *J. Am. Chem. Soc.*, 1968, **90**, 2001.
19 W. Gee, R. A. Shaw and B. C. Smith, *Inorg. Synth.*, 1967, **9**, 19.
20 S. C. Critchlow and J. D. Corbett, *J. Am. Chem. Soc.*, 1983, **105**, 5715.
21 D. R. Gardner, B. W. Eichhorn and B. Scott, results to be published.
22 R. A. Jones, A. Stuart, J. L. Atwood, W. E. Hunter and R. D. Rogers, *Organometallics*, 1982, **1**, 1721.
23 R. A. Jones, A. Stuart, J. L. Atwood and W. E. Hunter, *Organometallics*, 1983, **2**, 874.
24 R. A. Jones, N. C. Norman, M. H. Seeberger, J. L. Atwood and W. E. Hunter, *Organometallics*, 1983, **2**, 1629.
25 A. J. Carty, S. A. Maclaughlin and D. Nucciarone, *Phosphorus-31 NMR Stereochemical Analysis*, ed. J. G. Verkade and L. D. Quin, VCH, New York, 1987.
26 J. P. Collman, R. K. Rothrock, R. G. Finke, E. J. Moore and F. Rose-Munch, *Inorg. Chem.*, 1982, **21**, 146.
27 S. Charles, S. G. Bott, A. L. Rheingold and B. W. Eichhorn, *J. Am. Chem. Soc.*, 1994, **116**, 8077.
28 S. Ya, *EPR of Free Radicals*, Wiley, New York, 1974.
29 G. M. Sheldrick, SHELXTL, Siemens Analytical X-ray Instruments, Inc., Madison, WI, 1994.
30 G. Sheldrick, *Acta. Crystallogr.*, *Sect. A*, 1990, **46**, 467.
31 C. K. Johnson, ORTEP, Report ORNL-5138, Oak Ridge National Laboratory, Oak Ridge, TN, 1976.